HemaSphere

EHA EUROPEAN HEMATOLOGY ASSOCIATION

Article
Open Access

CSF3R T618I Collaborates With RUNX1-RUNX1T1 to Expand Hematopoietic Progenitors and Sensitizes to GLI Inhibition

Anja S. Swoboda[1,2,3], Vanessa C. Arfelli[1,2,3], Anna Danese[4,5], Roland Windisch[6], Paul Kerbs[1,2,3], Enric Redondo Monte[1,2,3], Johannes W. Bagnoli[7], Linping Chen-Wichmann[6], Alessandra Caroleo[1,2,3], Monica Cusan[1,2,3], Stefan Krebs[8], Helmut Blum[8], Michael Sterr[9,10], Wolfgang Enard[7], Tobias Herold[1,2,3], Maria Colomé-Tatché[4,11], Christian Wichmann[6], Philipp A. Greif[1,2,3]

GRAPHICAL ABSTRACT

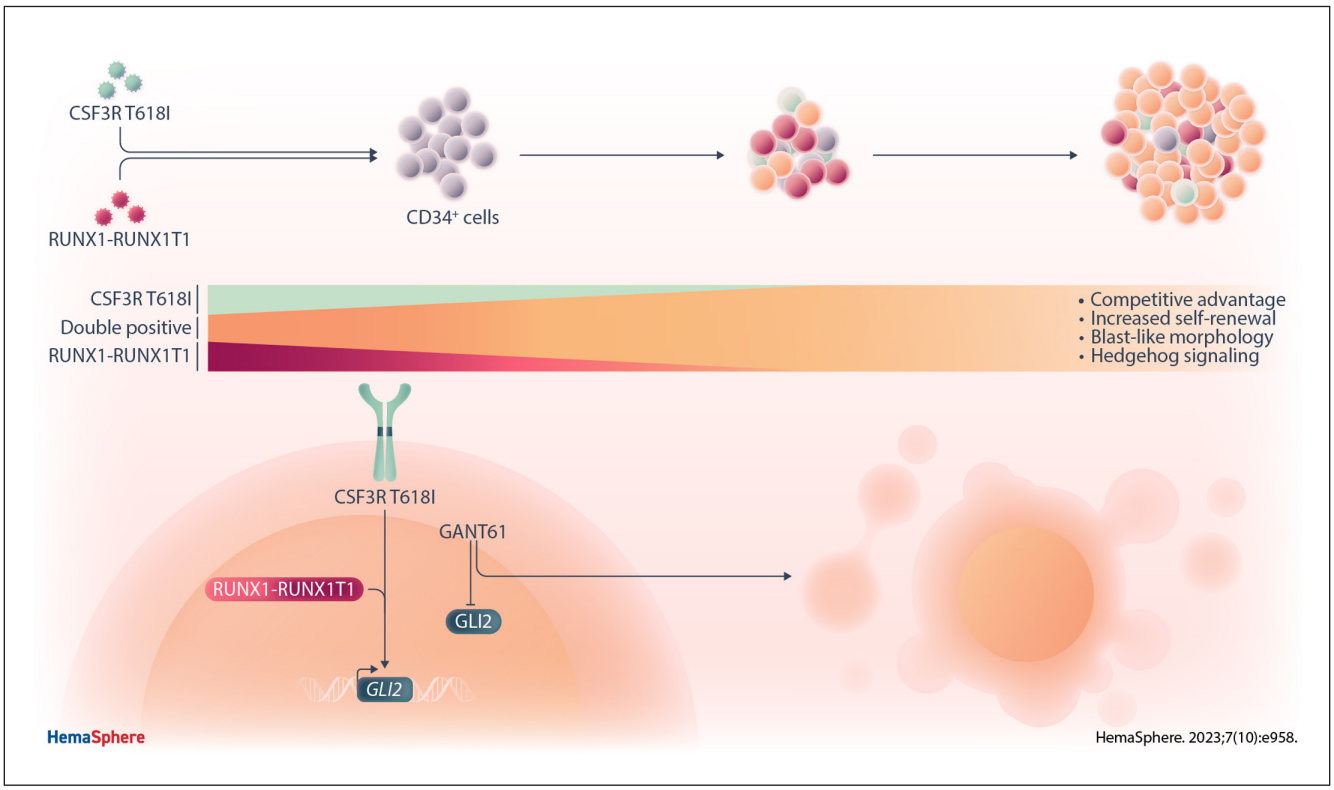

HemaSphere

EHA EUROPEAN HEMATOLOGY ASSOCIATION

Article
Open Access

CSF3R T618I Collaborates With RUNX1-RUNX1T1 to Expand Hematopoietic Progenitors and Sensitizes to GLI Inhibition

Anja S. Swoboda[1,2,3], Vanessa C. Arfelli[1,2,3], Anna Danese[4,5], Roland Windisch[6], Paul Kerbs[1,2,3], Enric Redondo Monte[1,2,3], Johannes W. Bagnoli[7], Linping Chen-Wichmann[6], Alessandra Caroleo[1,2,3], Monica Cusan[1,2,3], Stefan Krebs[8], Helmut Blum[8], Michael Sterr[9,10], Wolfgang Enard[7], Tobias Herold[1,2,3], Maria Colomé-Tatché[4,11], Christian Wichmann[6], Philipp A. Greif[1,2,3]

Correspondence: Philipp A. Greif (pgreif@med.lmu.de).

ABSTRACT

Activating colony-stimulating factor-3 receptor gene (*CSF3R*) mutations are recurrent in acute myeloid leukemia (AML) with t(8;21) translocation. However, the nature of oncogenic collaboration between alterations of *CSF3R* and the t(8;21) associated *RUNX1-RUNX1T1* fusion remains unclear. In CD34+ hematopoietic stem and progenitor cells from healthy donors, double oncogene expression led to a clonal advantage, increased self-renewal potential, and blast-like morphology and distinct immunophenotype. Gene expression profiling revealed hedgehog signaling as a potential mechanism, with upregulation of *GLI2* constituting a putative pharmacological target. Both primary hematopoietic cells and the t(8;21) positive AML cell line SKNO-1 showed increased sensitivity to the GLI inhibitor GANT61 when expressing *CSF3R* T618I. Our findings suggest that during leukemogenesis, the *RUNX1-RUNXT1* fusion and *CSF3R* mutation act in a synergistic manner to alter hedgehog signaling, which can be exploited therapeutically.

INTRODUCTION

Somatic mutations of the colony-stimulating factor-3 receptor (*CSF3R*) gene in acute myeloid leukemia (AML) are highly associated with alterations of hematopoietic transcription factors, such as core binding factor (CBF) abnormalities or *CEBPA* double mutations.[1–3] In particular, we and others found proximal membrane domain mutations of *CSF3R*, represented by the hotspot alteration T618I, either in t(8;21) positive CBF leukemia or *CEBPA* double mutated AML.[4–6] *CSF3R* T618I was initially described in chronic neutrophilic leukemia (CNL) and atypical chronic myeloid leukemia (aCML).[4,7] Proximal membrane mutations of *CSF3R* lead to ligand independent receptor activation with disrupted differentiation and proliferative advantage. While the presence of the t(8;21) associated fusion gene *RUNX1-RUNX1T1* in AML generally indicates a favorable prognosis, we lack understanding of the role of *CSF3R* mutations during AML development and treatment outcome. RUNX1-RUNX1T1 (also known as AML1-ETO) leads to partial block of myeloid differentiation, but is not sufficient to cause leukemia alone, indicating the requirement of additional genetic lesions.[8–11] The cooperation between alterations in hematopoietic transcription factors and signaling cascades leads to block of differentiation and increased proliferation, which represents a classical model of leukemogenesis.[12,13] In the present study, we investigated the oncogenic collaboration between the RUNX1-RUNX1T1 fusion and the CSF3R mutant T618I and found that—beyond disturbing differentiation and driving proliferation in a complementary manner—they may synergistically activate specific pathways.

METHODS

Plasmids

The expression vector pMSCV-RUNX1-RUNX1T1TR-IRES-tdTomato has been described previously.[14] Expression vectors pMSCV-IRES-GFP with CSF3R wild type and T618I mutant,

[1]Department of Medicine III, University Hospital, LMU Munich, Germany
[2]German Cancer Consortium (DKTK), Partner Site Munich, Germany
[3]German Cancer Research Center (DKFZ), Heidelberg, Germany
[4]Computational Health Center, Helmholtz Center Munich, Neuherberg, Germany
[5]Department of Physiological Genomics, Biomedical Center Munich, Ludwig-Maximilians University, Germany
[6]Division of Transfusion Medicine, Cell Therapeutics and Haemostaseology, University Hospital, LMU Munich, Germany
[7]Anthropology and Human Genomics, Faculty of Biology, LMU Munich, Martinsried, Germany
[8]Gene Center - Laboratory for Functional Genome Analysis, LMU Munich, Germany
[9]Institute of Diabetes and Regeneration Research, Helmholtz Diabetes Center, Helmholtz Center Munich, Neuherberg, Germany
[10]German Center for Diabetes Research (DZD), Neuherberg, Germany
[11]Biomedical Center (BMC), Physiological Chemistry, Faculty of Medicine, LMU Munich, Planegg-Martinsried, Germany

Supplemental digital content is available for this article.

HemaSphere (2023) 7:10(e958).
http://dx.doi.org/10.1097/HS9.0000000000000958.
Received: October 17, 2022 / Accepted: August 22, 2023

and vector control were a generous gift from Julia Maxson, Portland, Oregon.[15]

Cell culture and retroviral transduction

SKNO-1 cells (DSMZ, ACC-690) were cultured in RPMI 1640 Glutamax (Invitrogen, Carlsbad, CA) supplemented with 10% fetal bovine serum (FBS) (PAN Biotech, Aidenbach, Germany), 1% penicillin-streptomycin (PAN biotech), and 10 ng/mL granulocyte-macrophage colony stimulating factor (GM-CSF) (Miltenyi Biotech, Bergisch Gladbach, Germany). HEK 293T cells (DSMZ, ACC-635) were cultured in Dulbecco's modified Eagle's medium (PAN Biotech) supplemented with 10% FBS and 1% penicillin-streptomycin. CD34+ bone marrow cells (Lonza, Basel, Switzerland) were cultured in Iscove's modified Dulbecco's medium (Gibco, Carlsbad, CA), supplemented with 20% FBS, 1% penicillin-streptomycin, 4 µM L-Glutamine (Gibco), 10 ng/mL interleukin (IL)-3, 20 ng/mL IL-6, 20 ng/mL Flt3-L, 20 ng/mL GM-CSF, 20 ng/mL stem cell factor, and 20 ng/mL thrombopoietin (cytokines were obtained from Peprotech, Hamburg, Germany). Retroviral transduction of CD34+ cells was performed as described before.[14,16] Transduction of SKNO-1 was performed accordingly with the culture medium described above.

Flow cytometry

Beginning 4 days posttransduction, CD34+ progenitor cells were analyzed every 2–3 days for expression of tdTomato and enhanced green fluorescent protein (GFP) by flow cytometry. SKNO-1 cells were either sorted 10 days after transduction or left unsorted.

For analysis of cell surface marker expression, allophycocyanin (APC)-, phycoerythrin/cyanine 7 (PE/Cy7)-, or PE-Vio770-conjugated anti-human HLA-DR, CD3, CD10, CD11b, CD11c, CD13, CD14, CD15, CD18, CD19, CD27, CD33, CD34, CD41a, CD49a, CD117, and CD135 antibodies were used (BioLegend, San Diego, CA; BD Life Sciences, Franklin Lakes, NJ; or Miltenyi Biotech, Bergisch Gladbach, Germany). Isotype controls mouse IgG1, mouse IgG2a, mouse IgM, and recombinant human IgG1 were used accordingly. CSF3R localization was evaluated in permeabilized SKNO-1 cells using PE-conjugated (intracellular) or APC-conjugated (surface) anti-human CD114 antibody (Miltenyi Biotech, Bergisch Gladbach, Germany). Mouse IgG1, k isotype controls for PE and APC (BD Biosciences, Franklin Lakes, NJ) were used as control.

Apoptosis rates were measured by flow cytometry following cell staining with APC-conjugated Annexin V (BD Pharmingen, Franklin Lakes, NJ) according to the manufacturer's recommendations in combination with 4',6-diamidino-2-phenylindole (DAPI) as vital dye.

Cell cycle was assessed by flow cytometry after DRAQ5 staining (Alexis Biochemicals, San Diego, CA) for 10 minutes at 37°C.

All flow cytometry experiments were performed using FACS Calibur or FACS Canto II (BD Life Sciences). Data were analyzed using FlowJo Software (BD Life Sciences). Statistical analysis was performed using GraphPad Prism (GraphPad Software Inc., San Diego, CA). *P*-values were calculated using the student *t* test.

Cytotoxicity assay

SKNO-1 or progenitor cells (3×10^4/well) were treated in 96-well plates for 72 hours with varying concentrations of Janus kinase (JAK) inhibitor ruxolitinib phosphate (ChemScene, Monmoth Junction, NJ), STAT3 inhibitor XIII, C188-9 (EMD Millipore, Billerica, MA), GLI inhibitor GANT61 (TOCRIS, Bristol, UK), or the multikinase (BCR-ABL/SRC) inhibitor dasatinib (Santa Cruz Biotechnology, Dallas, TX). Sixty-eight hours posttreatment, 20 µL of CellTiter-Blue reagent was added to each well of cells as recommended by the manufacturer. Plates were incubated for additional 4 hours at 37°C in the dark. Readout was obtained using the CellTiter-Blue Cell Viability Assay protocol with the GloMax Discover plate reader (both from Promega, Fitchburg, WI). Three independent experiments, each consisting of 3 technical replicates for the single-drug concentrations, were performed for the inhibitors tested. Analysis was carried out in GraphPad Prism (GraphPad Software Inc., San Diego, CA). Values were normalized to the dimethyl sulfoxide control (drug solvent) and drug response was assessed by nonlinear regression (curve fit) using the equation: "log (inhibitor) versus normalized response – variable slope".

Bulk and single-cell RNA sequencing

Human progenitor cells double transduced with *RUNX1-RUNX1T1*tr and *CSF3R* WT or T618I were submitted to bulk RNA sequencing (Prime-seq) at day 60 of outgrowth. Library preparation, sequencing, analysis of differential gene expression, and pathway analysis were performed as described before.[16–18] For single-cell RNA sequencing (scRNA-seq), libraries from cells harvested on day 30 and 60 were prepared using the Chromium Next GEM Single Cell 3′ GEM Kit v3.1 (10× Genomics, Pleasanton, CA) according to the manufacturer's instructions. Paired-end sequencing (Read 1: 28bp; Read 2: 91bp) was performed on an Illumina HiSeq 1500 instrument, with an average of 50,000 reads per cell and 10,000 cells per library. Sample demultiplexing and alignment of the data were done using the Cell Ranger software (v6.1.2) and the human genome GRCh38.p13 from Gencode (release 39). Further data processing (quality control, filtering, normalization, highly variable gene selection, embedding, and visualization) was performed using the python package scanpy v1.9.1.[19] We filtered cell barcodes with <3000 counts, >100,000 counts, or >20% of mitochondrial reads. Additionally, we removed cells with >600 genes captured. It resulted in 29,781 cells and 30,039 genes across 4 samples (at day 30: 7530 cells for *CSF3R* WT and 7661 cells for *CSF3R* T618I; at day 60: 6432 cells for *CSF3R* WT and 8158 cells for *CSF3R* T618I, respectively). Finally, the cell type annotation was done using the package CellTypist v1.3.1.[20] The notebooks used for the scRNA-seq analysis are available on Github (https://github.com/colomemaria/CSF3R_scRNAseq_reproducibility).

RESULTS

CSF3R T618I confers a clonal advantage to RUNX1-RUNX1T1 expressing progenitors

We set out to study the role of the activating *CSF3R* mutation T618I in a *RUNX1-RUNX1T1* positive background, using CD34+ hematopoietic stem and progenitor cells (HSPCs) from adult healthy donors (Figure 1A). While expression of a truncated form of the t(8;21) related RUNX1-RUNX1T1 (RUNX1-RUNX1T1tr) fusion is sufficient to expand hematopoietic progenitor cells, we observed that coexpression of the CSF3R mutant T618I (CSF3R T618I) but not CSF3R wild type (WT) led to competitive outgrowth of cells (Figure 1B; Suppl. Figure S1A-S1C). In contrast, overexpression of either CSF3R WT or CSF3R T618I alone did not lead to considerable cell expansion (Suppl. Figure S1D). The *CSF3R* single transduced hematopoietic progenitor cells started to differentiate and lost their proliferative potential within 1 month (data not shown).

CSF3R T618I induces an immunophenotype resembling acute myelomonocytic leukemia

After ex vivo expansion, cells were analyzed via flow cytometry for surface expression of differentiation markers. Only a minor subpopulation of RUNX1-RUNX1T1tr single positive cells showed surface expression of CD34, while most cells expressed myeloid markers, consistent with previous reports.[11,14,21] CSF3R T618I coexpressing cells were negative for

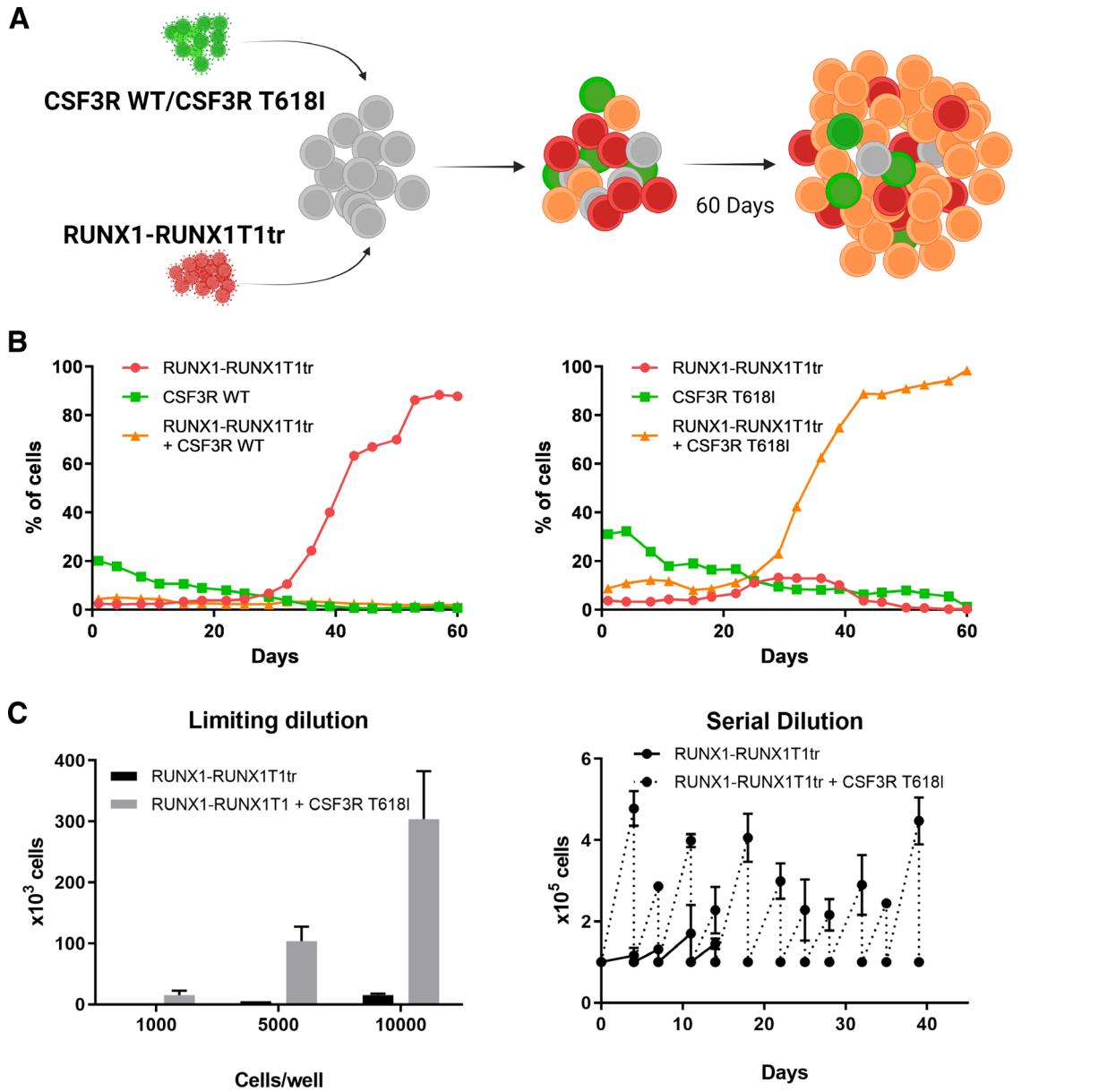

Figure 1. CSF3R T618I collaborates with RUNX1-RUNX1T1tr to expand HSPCs. (A) Schematic outline of the experimental setup. hCD34+ cells were virally transduced with CSF3R WT or T618I (GFP) and RUNX1-RUNX1T1tr (tdTomato). Competitive growth was assessed by flow cytometry every 2–3 d over a period of 60 d. (B) Flow cytometry measurement of one representative competitive growth assay. (C) Limiting dilution assay: indicated cell numbers of transduced hCD34+ cells were seeded after expansion. Cell number was assessed 11 d post seeding (left). Serial dilution: 1×10^5 transduced hCD34+ cells were seeded after expansion. Cells were counted every 2–3 d and reseeded at initial cell number (right). Error bars represent ±SEM. CSF3R = colony-stimulating factor-3 receptor; HSPC = hematopoietic stem and progenitor cells; WT = wild type.

CD34, but highly positive for the pan-myeloid marker CD13 and the monocytic marker CD14. In addition, double positive cells expressed HLA-DR, CD11b, CD11c, CD33, CD18, and partly CD49a (Suppl. Figure S2). A similar immunophenotype was reported in monocytic cells, including monoblasts and promonocytes, of patients with acute myelomonocytic leukemia (AMML).[22–24]

CSF3R T618I leads to increased self-renewal and blast morphology

Because self-renewal potential and increased proliferation frequency are key mechanisms in leukemogenesis, we performed limiting and serial dilution experiments. Seeding low numbers of RUNX1-RUNX1T1tr single positive cells did not result in measurable proliferation after 7 or 11 days, whereas seeding of 1×10^4 cells resulted in an increase of cell number by 50% after 11 days. Analysis of double oncogene expressing cells 11 days post seeding revealed an average increase of cell number by 15-fold to 30-fold (Figure 1C, left panel). Serial dilution to 1×10^5 cells showed highly increased proliferation and self-renewal potential in double oncogene expressing cells as compared with RUNX1-RUNX1T1tr single positive cells (Figure 1C, right panel).

To mimic the subsequent acquisition of genetic lesions required for leukemic transformation, we next transduced naive HSPCs with *RUNX1-RUNX1T1*tr alone. Thereby, the cells clonally expanded, resulting in a culture composed of >95% fluorescence-marker positive cells. Next, we introduced a second hit by superinfection with the retroviral *CSF3R* T618I construct (Figure 2A). This led to complete outgrowth of double positive cells over a period of another 60 days (Figure 2B). The cytomorphology analysis showed a heterogeneous mixture

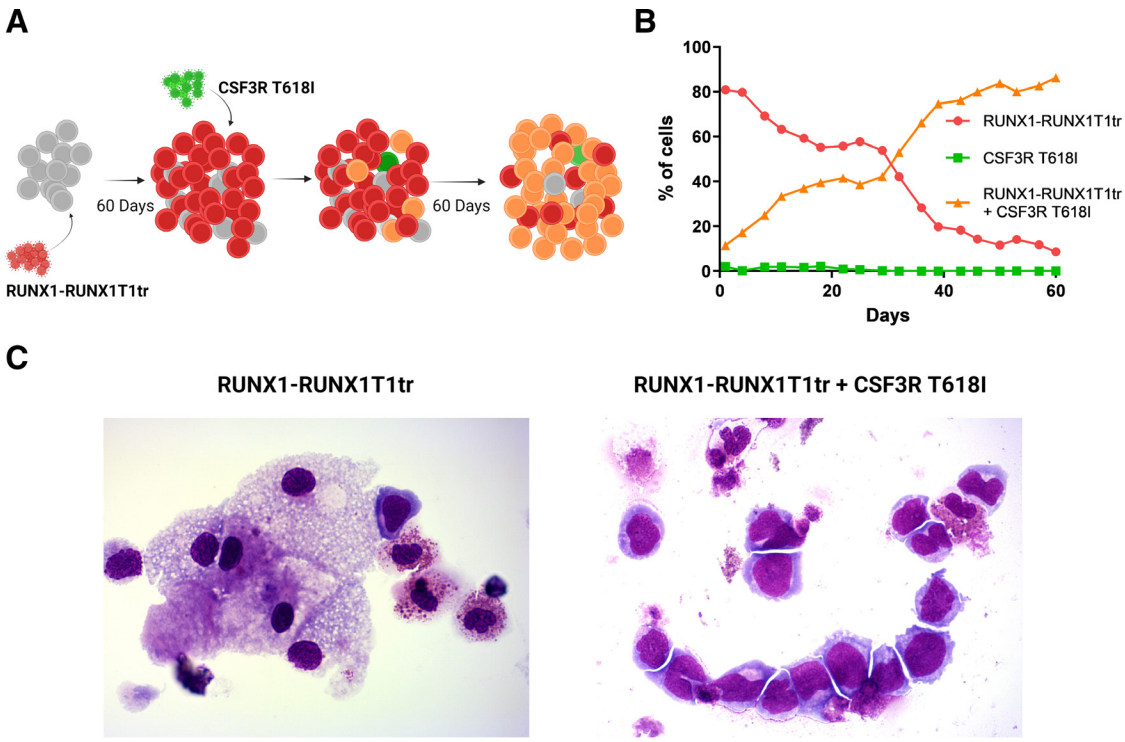

Figure 2. Forced expression of CSF3R T618I in a RUNX1-RUNX1T1tr background provides a competitive advantage and induces blast morphology. (A) Schematic outline of the experimental setup. hCD34+ cells were virally transduced with RUNX1-RUNX1T1tr and expanded over the period of 60 d. Expansion of tdTomato-positive cells was assessed every 2–3 d by flow cytometry. Post expansion, hCD34+ cells were superinfected with CSF3R WT or T618I. Competitive growth was assessed by flow cytometry every 2–3 d over a period of another 60 d. (B) Flow cytometry measurement of one representative competitive growth assay after superinfection. (C) Morphological analyses of cytospin/Giemsa preparations of hCD34+ cells 60 d post superinfection. CSF3R = colony-stimulating factor-3 receptor; WT = wild type.

of mature and immature cells in RUNX1-RUNX1T1tr single positive cells, whereas double positive cells remained mostly undifferentiated, featuring a homogeneous blast-like morphology (Figure 2C).

CSF3R T618I and RUNX1-RUNX1T1 synergistically alter specific pathways

Next, we analyzed the differential gene expression between single and double oncogene expressing primary HSPCs upon outgrowth (day 60, n = 6/group). RNA sequencing by Prime-seq[18] revealed a significant deregulation of 626 genes upon expression of *CSF3R* T618I (Figure 3A; Suppl. Table S1). Pathway analysis showed alteration of folate and pterin metabolism, a central mechanism of nucleotide synthesis and DNA methylation. Furthermore, signaling pathways of IL-10, IL-4, and IL-13 were upregulated, all known to have anti-inflammatory properties on immune cells. Interestingly, also the hedgehog signaling pathway was significantly enriched (Figure 3B) with *GLI2* being among the most prominently upregulated genes upon *CSF3R* T618I expression (Figure 3A and 3C). Consistent with previous reports,[25] we observed shorter overall survival in patient samples of the German Acute Myeloid Leukemia Cooperative Group (AMLCG)-2008 trial (Figure 3D). In gene expression data from Beat-AML patients, we confirmed upregulation of *GLI2* in patients harboring *FLT3*-ITD (Suppl. Figure S3A). Of note, within the Beat-AML cohort, we found elevated levels of *GLI2* expression in AML patients with *CSF3R* mutations, similar to AML with *FLT3*-ITD (Suppl. Figure S3B; Suppl. Table S2).

We next performed single-cell RNA-seq in order to evaluate the dynamic changes in the double transduced cell populations over time (Suppl. Figure S4). Upon outgrowth (day 60), a representative culture with CSF3R T618I-mediated expansion of double positive cells showed more immature hematopoietic stem and multipotent progenitor cells (HSC/MPP) compared with the culture with RUNX1-RUNX1T1tr-mediated expansion of single positive cells and cotransduction with *CSF3R* WT (Figure 4A; Suppl. Figure S4b). This is in line with the cytomorphology featuring predominantly blast-like cells in the double positive culture (Figure 2C). Furthermore, *GLI2* expression was enriched in the HSC/MPP compartment and in the macrophage-committed progenitors, the two most abundant cell types within the *CSF3R* T618I transduced culture (Figure 4B and 4C).

CSF3R T618I confers cytokine independence in the t(8;21)-positive cell line SKNO-1

Previous studies in murine t(8;21) models have shown that preleukemic clones, expanded by RUNX1-RUNX1T1, are highly cytokine dependent, suggesting that mutations leading to cytokine-mediated survival and proliferation advantages might be crucial collaborators in leukemogenesis.[11,21,26,27] Therefore, we conducted further experiments in the GM-CSF dependent t(8;21)-positive cell line SKNO-1, where we observed cytokine independent growth in the presence of CSF3R T618I but not CSF3R WT (Figure 5A). GM-CSF withdrawal of SKNO-1 native cells, vector control, or CSF3R WT expressing cells led to cell cycle arrest that could be overcome by expression of CSF3R T618I (Figure 5B). Because activation of the receptor by its ligand G-CSF physiologically requires dimerization and internalization, we sought to characterize surface and intracellular abundance of CSF3R. SKNO-1 cells overexpressing CSF3R WT showed higher levels of receptor protein on the surface. In contrast, overexpressed CSF3R T618I localized predominantly in the intracellular compartment, while the ratio of surface to

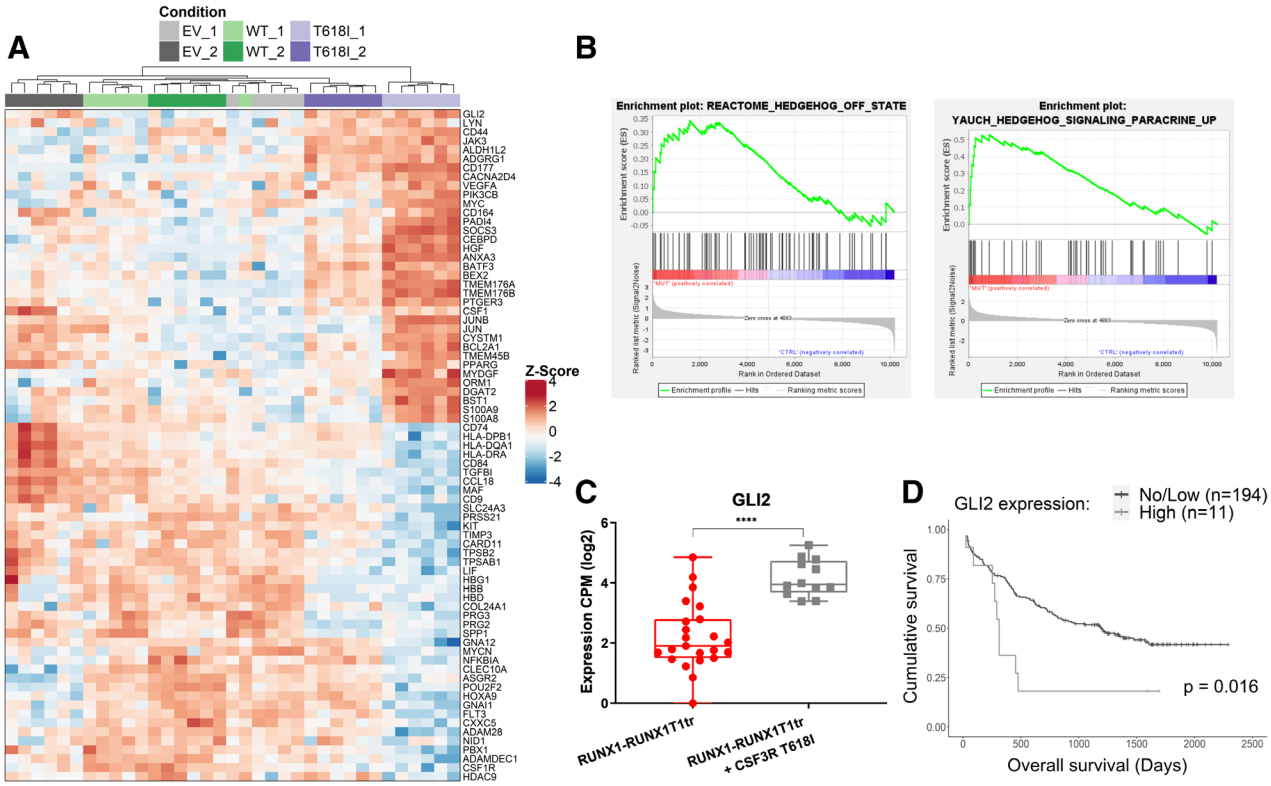

Figure 3. CSF3R T618I induces Hedgehog signaling. (A) Heat map of significantly ($P < 0.05$) deregulated genes in hCD34+ cells after 60 d of competitive outgrowth with *RUNX1-RUNX1T1*tr and *CSF3R* T618I compared with cotransduction of vector control (EV) or *CSF3R* WT. Data was obtained after performance of bulk RNA-seq (Prime-Seq) analysis. (n = 2 independent transductions/construct; n = 6 replicates/transduction). (B) GSEA of RNA-seq data shows enrichment of hedgehog signaling genes in CSF3R T618I expressing cells. (C) GLI2 expression as obtained from RNA-seq. Replicates of outgrown RUNX1-RUNX1T1tr populations (in red) resulting from double transduction with *CSF3R* WT (n = 12) and pMIG EV (n = 11) were pooled together for this analysis, as they behave similarly in the growth competition assay. Differential expression analysis was performed with edgeR/limma package (****$P < 0.0001$). (D) OS according to *GLI2* expression of patients enrolled in the AMLCG-2008 study cohort (GSE106291). High expression was considered n(Transcripts) ≥1; low/no expression was considered n(Transcripts) <1. CSF3R = colony-stimulating factor-3 receptor; GSEA = gene set enrichment analysis; OS = overall survival; WT = wild type.

intracellular localization did not differ markedly from endogenous CSF3R (Suppl. Figure S5).

CSF3R T618I sensitizes to GLI inhibition in a RUNX1-RUNX1T1 background

Subsequently, we investigated pharmacological counteraction of CSF3R T618I through inhibition of putative downstream effectors. Therefore, we used GANT61 to treat outgrown HSPCs that express RUNX1-RUNX1T1tr in combination with either CSF3R WT or CSF3R T618I. Expression of CSF3R T618I significantly sensitized the cells to GLI inhibition (Figure 5C; right panel).

Independently, we confirmed that CSF3R T618I expressing SKNO-1 cells were as well significantly more sensitive toward treatment with GANT61, as compared with CSF3R WT control (Figure 5C; left panel). Considering previously reported signal transduction of mutated CSF3R via JAK2 and STAT3,[7] we also tested the JAK2 inhibitor ruxolitinib and the STAT3 inhibitor C188-9. Pharmacological targeting of either of the two downstream effectors did not show increased sensitivity upon ectopic expression of *CSF3R* T618I compared with WT (Suppl. Figure S6A and S6B). Remarkably, Western Blot analysis showed enhanced phosphorylation of STAT3 for CSF3R T618I as compared with CSF3R WT or vector control, whereas JAK2 protein expression was highly decreased with no measurable phosphorylation (Suppl. Figure S6D). Interestingly, CSF3R T618I conferred a slightly increased sensitivity to the multikinase inhibitor dasatinib (Suppl. Figure S6C).

DISCUSSION

Although the *CSF3R* mutation T618I has been investigated extensively in the context of CNL and aCML,[7,28–30] its role in AML is mainly described in conjunction with *CEBPA* mutation.[31] In a first step, we were able to shed light on the importance of the *CSF3R* mutation T618I in clonal competition during leukemogenesis. It is widely believed that the RUNX1-RUNX1T1 fusion leads to enhanced self-renewal potential and blockade of various differentiation pathways, thus expanding early progenitor cells.[8,10,11,21,32] Markedly, hematopoietic progenitor cells retrovirally expressing *RUNX1-RUNX1T1* reportedly do not promote leukemia in immunodeficient mice.[8–11] While treatment with G-CSF has been shown to increase cell proliferation significantly upon expression of RUNX1-RUNX1T1,[33] leukemogenesis only occurs in the presence of secondary mutations.[8,10,27,34–37] According to the classical two-hit model, leukemogenesis in AML requires a block of differentiation on the one hand and increased proliferative advantage on the other.[12] In accordance with the literature, we were able to expand hematopoietic stem and progenitor cells by ectopically expressing RUNX1-RUNX1T1tr, leading to blockage of differentiation. Interestingly, CSF3R T618I not only enhanced proliferation and provided cytokine independent cell cycle progression but also generated immature cell populations with even higher frequency of cells with self-renewal potential and increased survival potential. Thus, CSF3R T618I does not only serve as a classical proliferation driver in our setting, but also further aggravates the block of differentiation. Coexpression of RUNX1-RUNX1T1tr and CSF3R

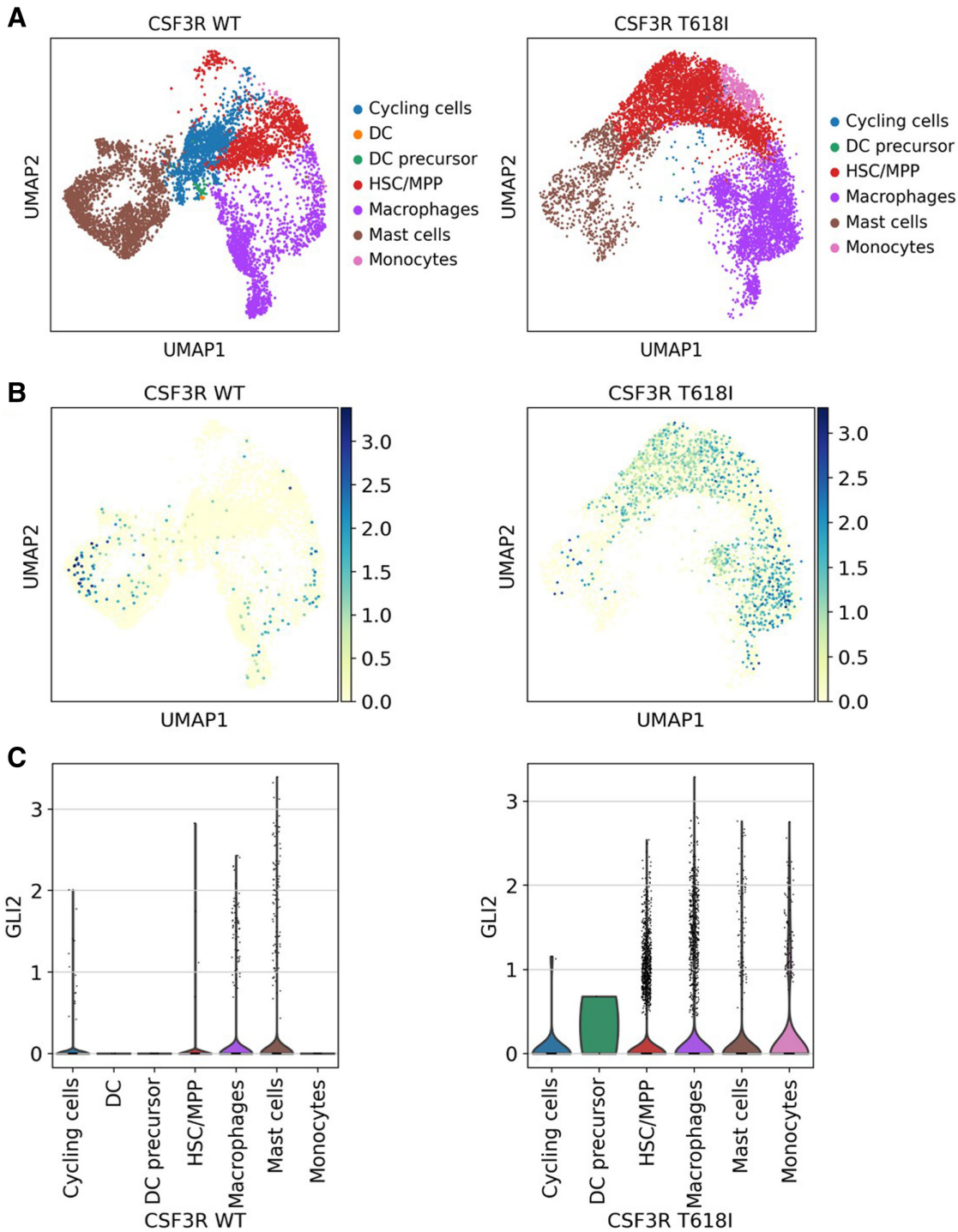

Figure 4. Single-cell RNA-seq shows enrichment of immature hematopoietic cells (HSC/MPP) and *GLI2* upregulation in the culture with CSF3R T618I-mediated expansion of double positive cells (day 60). (A) UMAP showing different subpopulations annotated with CellTypist for CSF3R WT or T618I. (B) UMAP showing *GLI2* expression for CSF3R WT or T618I. (C) Violin plots showing *GLI2* expression across the subpopulations for CSF3R WT or T618I. CSF3R = colony-stimulating factor-3 receptor; HSC/MPP = hematopoietic stem and multipotent progenitor cells; WT = wild type.

T618I highly resembled the phenotype of AMML, all together suggesting leukemic transformation.

CSF3R signaling has been proposed to involve phosphorylation of JAK2 and STAT3 in the context of CNL.[7] Furthermore, activating *JAK2* mutations are recurrently found in t(8;21) positive AML, suggesting a cooperative effect in leukemogenesis.[5,38–41] Interestingly, pharmacologic counteraction of both JAK2 and STAT3 signaling did not result in increased cell death upon expression of CSF3R T618I in our study. Here, we found a significant decrease in JAK2 protein abundance (Suppl. Figure S6D) that was not reflected in significant mRNA deregulation (Suppl. Figure S7A). This suggests both a posttranslational downregulation mechanism of JAK2, possibly by SOCS3[42,43] (Suppl. Figure S7C), and an alternative activation of STAT3 in presence of mutated CSF3R. The increased phosphorylation of STAT3 upon CSF3R T618I expression (Suppl. Figure

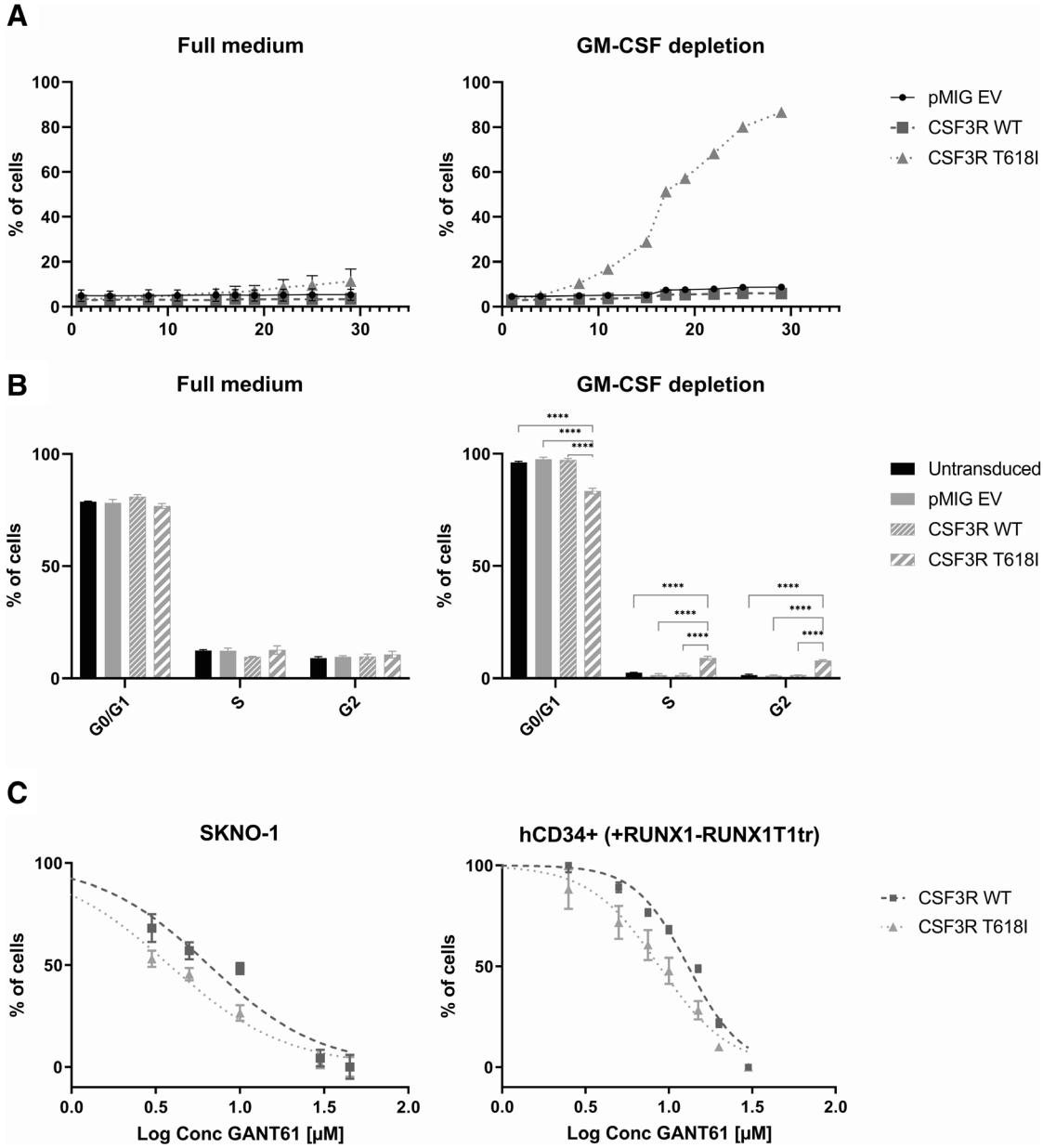

Figure 5. CSF3R T618I confers cytokine independence and increased sensitivity to GLI inhibition. (A) Competitive growth analysis of cell line SKNO-1 virally transduced with vector control (EV), *CSF3R* WT or T618I, cultivated with or without GM-CSF. Expression of fluorescent marker (GFP) was assessed every 2–3 d using flow cytometry. (B) Cell cycle analysis of SKNO-1 untransduced, transduced with vector control (EV), *CSF3R* WT or T618I, and cultured with or without GM-CSF. Cell cycle was assessed after staining with DRAQ5 and detection using flow cytometry. Cell cycle analysis was performed using FlowJo Software. Error bars represent ±SEM. Comparison was performed using two-tailed unpaired *t* test (*****P* < 0.0001). (C) GLI inhibition using escalating doses of GANT61 in sorted SKNO-1 (left) and expanded hCD34+ cells (right) transduced with CSF3R WT or T618I. CSF3R = colony-stimulating factor-3 receptor; GM-CSF = granulocyte-macrophage colony stimulating factor; WT = wild type.

S6D) points toward an alternative, possibly redundant signal transduction of mutated CSF3R in the context of t(8;21) AML. Alternative pathways might involve signaling via ERK[15,44] or a switch toward different members within the JAK family. This is supported by our RNA-seq results, where we found JAK3 significantly upregulated upon CSF3R T618I expression (Suppl. Figure S7B).

Remarkably, CSF3R T618I SKNO-1 cells were more sensitive to dasatinib, which is classically defined as a BCR-ABL and SRC family kinase inhibitor. STAT3 is one of the downstream targets of SRC signaling pathway; however, as STAT3 inhibition did not render the CSF3R T618I expressing cells more sensitive, signaling through the SRC kinases may involve other downstream effectors.[45]

As an alternative route, we observed that mutated *CSF3R* induces ligand independent signaling via the hedgehog pathway. In particular, we found the hedgehog downstream effector *GLI2* specifically upregulated upon coexpression of RUNX1-RUNX1T1 and CSF3R T618I. Of note, patient data and mouse models support a specific collaboration of upregulated *GLI2* and *FLT3*-ITD in AML.[25,46] *GLI2* expression is a negative prognostic marker in AML, associated with significantly shorter event-free and overall survival,[25] as we were able to confirm within the AMLCG patient cohort. The correlation between *GLI2* expression and overall survival is not limited to the CBF subgroup, suggesting a general mechanism in AML. Hedgehog pathway signaling plays a critical role in embryogenesis,

primitive embryonal hematopoiesis, and maintenance of hematopoietic stem cells and is tightly regulated.[47] Deregulation in AML might lead to development and expansion of chemotherapy resistant leukemic stem cells, promoting therapy resistance and relapse.[48,49] Thus, inhibition of hedgehog pathway signaling became a promising target. Recently, the smoothened (SMO) inhibitor glasdegib was approved both by the United States Food and Drug Administration (US FDA) and the European Medicines Agency (EMA) as the first hedgehog pathway inhibitor for treatment of AML patients in combination with low-dose cytarabine (Ara-C),[50,51] while further drugs are investigated. In preclinical studies, GLI inhibition by GANT61 caused apoptosis in Ara-C-resistant cells and sensitized to both Ara-C and rapamycin treatment.[48,52,53] Interestingly, targeting of the hedgehog pathway sensitized to dasatinib treatment in pancreatic cancer[54] and in leukemia cells.[55] In light of our results that CSF3R T618I sensitizes both to dasatinib and GANT61, it is tempting to speculate that dasatinib may also target hedgehog signaling components, especially taking into account the reported crosstalk between hedgehog and the SRC downstream effector PI3K/AKT.[56] Maxson and colleagues (2013) found that patient-derived cells with CSF3R T618I were resistant to dasatinib. Although the KIT N822K mutation in the SKNO-1 cells might be a potential confounder in our study, since it is reported that this mutation can render these cells more sensitive to dasatinib,[57] the increased sensitivity upon expression of CSF3R T618I to this drug is specific. Several studies reported a broad target profile and recognized that dasatinib's antitumor activity is linked to its promiscuous nature in different cancers.[58–61] Therefore, the interplay between hedgehog signaling and potential context-specific targets of dasatinib needs further investigation.

Taken together, we have developed a human in vitro model for clonal competition mimicking the onset and progression of leukemic transformation. Our experiments provide evidence for the oncogenic collaboration between RUNX1-RUNX1T1 and CSF3R T618I via increased hedgehog signaling, which could be counteracted by GLI inhibition. This novel mechanism was confirmed in two independent model systems, namely the cell line SKNO-1 and primary hematopoietic stem and progenitor cells. Considering its upregulation in *FLT3*-ITD positive AML and upon presence of pathogenic *CSF3R* mutations, the downstream effector GLI2 becomes an increasingly attractive target for pharmacological intervention in AML.

AUTHOR CONTRIBUTIONS

ASS, LC-W, WE, CW, MC, and PAG designed the study. ASS, VCA, RW, ERM, TH, SK, HB, and MS performed research. ASS, RW, JWB, and AC collected data. ASS, VCA, PAG, and CW interpreted data. AD and PK performed bioinformatics analysis. JWB and MC-T provided bioinformatics support. AS performed statistical analysis. ASS, VCA, and PAG wrote the article.

DATA AVAILABILITY

The transcript expression data from this study are available in the Gene Expression Omnibus (GEO) repository, accession numbers GSE230755 (bulk Prime-seq) and GSE232187 (single-cell RNA-seq).

DISCLOSURES

The authors have no conflicts of interest to disclose.

SOURCES OF FUNDING

This study was supported by the German Research Foundation (DFG) within the Collaborative Research Centre (SFB) 1243 "Cancer Evolution" (Projects A08, A14, and Z02). PAG and CW acknowledge support by the Wilhelm Sander-Stiftung (Förderantrag Nr. 2014.162.3). PAG received funds from the Munich Clinician Scientist Program (MCSP) Advanced Track. MC-T and AD acknowledge the "Initiative and Networking Fund" of the Helmholtz Association (grant VH-NG-1219 for MC-T). AD received funds of the German Research Foundation (DFG STR 1385/5-1).

REFERENCES

1. Tarlock K, Alonzo T, Wang YC, et al. Prognostic impact of CSF3R mutations in favorable risk childhood acute myeloid leukemia. *Blood*. 2020;135:1603–1606.
2. Zhang Y, Wang F, Chen X, et al. CSF3R mutations are frequently associated with abnormalities of RUNX1, CBFB, CEBPA, and NPM1 genes in acute myeloid leukemia. *Cancer*. 2018;124:3329–3338.
3. Konstandin NP, Pastore F, Herold T, et al. Genetic heterogeneity of cytogenetically normal AML with mutations of CEBPA. *Blood Adv*. 2018;2:2724–2731.
4. Maxson JE, Ries RE, Wang YC, et al. CSF3R mutations have a high degree of overlap with CEBPA mutations in pediatric AML. *Blood*. 2016;127:3094–3098.
5. Opatz S, Bamopoulos SA, Metzeler KH, et al. The clinical mutatome of core binding factor leukemia. *Leukemia*. 2020;34:1553–1562.
6. Christen F, Hoyer K, Yoshida K, et al. Genomic landscape and clonal evolution of acute myeloid leukemia with t(8;21): an international study on 331 patients. *Blood*. 2019;133:1140–1151.
7. Maxson JE, Gotlib J, Pollyea DA, et al. Oncogenic CSF3R mutations in chronic neutrophilic leukemia and atypical CML. *N Engl J Med*. 2013;368:1781–1790.
8. Okuda T, Cai Z, Yang S, et al. Expression of a knocked-in AML1-ETO leukemia gene inhibits the establishment of normal definitive hematopoiesis and directly generates dysplastic hematopoietic progenitors. *Blood*. 1998;91:3134–3143.
9. Rhoades KL, Hetherington CJ, Harakawa N, et al. Analysis of the role of AML1-ETO in leukemogenesis, using an inducible transgenic mouse model. *Blood*. 2000;96:2108–2115.
10. Peterson LF, Zhang DE. The 8;21 translocation in leukemogenesis. *Oncogene*. 2004;23:4255–4262.
11. Mulloy JC, Cammenga J, Berguido FJ, et al. Maintaining the self-renewal and differentiation potential of human CD34+ hematopoietic cells using a single genetic element. *Blood*. 2003;102:4369–4376.
12. Kelly LM, Gilliland DG. Genetics of myeloid leukemias. *Annu Rev Genomics Hum Genet*. 2002;3:179–198.
13. Grimwade D, Ivey A, Huntly BJP. Molecular landscape of acute myeloid leukemia in younger adults and its clinical relevance. *Blood*. 2016;127:29–41.
14. Wichmann C, Quagliano-Lo Coco I, Yildiz O, et al. Activating c-KIT mutations confer oncogenic cooperativity and rescue RUNX1/ETO-induced DNA damage and apoptosis in human primary CD34+ hematopoietic progenitors. *Leukemia*. 2015;29:279–289.
15. Maxson JE, Luty SB, MacManiman JD, et al. Ligand independence of the T618I mutation in the colony-stimulating factor 3 receptor (CSF3R) protein results from loss of O-linked glycosylation and increased receptor dimerization. *J Biol Chem*. 2014;289:5820–5827.
16. Redondo Monte E, Wilding A, Leubolt G, et al. ZBTB7A prevents RUNX1-RUNX1T1-dependent clonal expansion of human hematopoietic stem and progenitor cells. *Oncogene*. 2020;39:3195–3205.
17. Bagnoli JW, Ziegenhain C, Janjic A, et al. Sensitive and powerful single-cell RNA sequencing using mcSCRB-seq. *Nat Commun*. 2018;9:2937.
18. Janjic A, Wange LE, Bagnoli JW, et al. Prime-seq, efficient and powerful bulk RNA sequencing. *Genome Biol*. 2022;23:88.
19. Wolf FA, Angerer P, Theis FJ. SCANPY: large-scale single-cell gene expression data analysis. *Genome Biol*. 2018;19:15.
20. Domínguez Conde C, Xu C, Jarvis LB, et al. Cross-tissue immune cell analysis reveals tissue-specific features in humans. *Science (1979)*. 2022;376:eabl5197.
21. Mulloy JC, Cammenga J, MacKenzie KL, et al. The AML1-ETO fusion protein promotes the expansion of human hematopoietic stem cells. *Blood*. 2002;99:15–23.
22. Xu Y, McKenna RW, Wilson KS, et al. Immunophenotypic identification of acute myeloid leukemia with monocytic differentiation. *Leukemia*. 2006;20:1321–1324.
23. Adriaansen HJ, te Boekhorst PA, Hagemeijer AM, et al. Acute myeloid leukemia M4 with bone marrow eosinophilia (M4Eo) and inv(16)(p13q22) exhibits a specific immunophenotype with CD2 expression. *Blood*. 1993;81:3043–3051.

24. Baer MR, Stewart CC, Lawrence D, et al. Acute myeloid leukemia with 11q23 translocations: myelomonocytic immunophenotype by multiparameter flow cytometry. *Leukemia*. 1998;12:317–325.
25. Wellbrock J, Latuske E, Kohler J, et al. Expression of hedgehog pathway mediator GLI represents a negative prognostic marker in human acute myeloid leukemia and its inhibition exerts Antileukemic effects. *Clin Cancer Res*. 2015;21:2388–2398.
26. Mulloy JC, Jankovic V, Wunderlich M, et al. AML1-ETO fusion protein up-regulates TRKA mRNA expression in human CD34+ cells, allowing nerve growth factor-induced expansion. *Proc Natl Acad Sci U S A*. 2005;102:4016–4021.
27. Yuan Y, Zhou L, Miyamoto T, et al. AML1-ETO expression is directly involved in the development of acute myeloid leukemia in the presence of additional mutations. *Proc Natl Acad Sci U S A*. 2001;98:10398–10403.
28. Foley A, Hughes SB, Meshinchi S, et al. CSF3R mutations synergize with CEBPA and SETBP1 mutations in acute myeloid leukemia and chronic neutrophilic leukemia. *Blood*. 2017;130(Suppl 1):3963.
29. Maxson JE, Tyner JW. Genomics of chronic neutrophilic leukemia. *Blood*. 2016;129:715–722.
30. Maxson JE, Fleischman AG, Luty SB, et al. CSF3R T618I mouse bone marrow transplant model of neutrophilic Leukemia. *Blood*. 2013;122:223.
31. Lavallée VP, Krosl J, Lemieux S, et al. Chemo-genomic interrogation of CEBPA mutated AML reveals recurrent CSF3R mutations and subgroup sensitivity to JAK inhibitors. *Blood*. 2016;127:3054–3061.
32. Tonks A, Pearn L, Tonks AJ, et al. The AML1-ETO fusion gene promotes extensive self-renewal of human primary erythroid cells. *Blood*. 2003;101:624–632.
33. Shimada H, Ichikawa H, Nakamura S, et al. Analysis of genes under the downstream control of the t(8;21) fusion protein AML1-MTG8: overexpression of the TIS11b (ERF-1, cMG1) gene induces myeloid cell proliferation in response to G-CSF. *Blood*. 2000;96:655–663.
34. de Guzman CG, Warren AJ, Zhang Z, et al. Hematopoietic stem cell expansion and distinct myeloid developmental abnormalities in a murine model of the AML1-ETO translocation. *Mol Cell Biol*. 2002;22:5506–5517.
35. Yergeau DA, Hetherington CJ, Wang Q, et al. Embryonic lethality and impairment of haematopoiesis in mice heterozygous for an AML1-ETO fusion gene. *Nat Genet*. 1997;15:303–306.
36. Schwieger M, Löhler J, Friel J, et al. AML1-ETO inhibits maturation of multiple lymphohematopoietic lineages and induces myeloblast transformation in synergy with ICSBP deficiency. *J Exp Med*. 2002;196:1227–1240.
37. Grisolano JL, O'Neal J, Cain J, et al. An activated receptor tyrosine kinase, TEL/PDGFbetaR, cooperates with AML1/ETO to induce acute myeloid leukemia in mice. *Proc Natl Acad Sci U S A*. 2003;100:9506–9511.
38. Schneider F, Bohlander SK, Schneider S, et al. AML1–ETO meets JAK2: clinical evidence for the two hit model of leukemogenesis from a myeloproliferative syndrome progressing to acute myeloid leukemia. *Leukemia*. 2007;21:2199–2201.
39. Schnittger S, Bacher U, Kern W, et al. JAK2 seems to be a typical cooperating mutation in therapy-related t(8;21)/ AML1-ETO-positive AML. *Leukemia*. 2007;21:183–184.
40. Lee JW, Kim YG, Soung YH, et al. The JAK2 V617F mutation in de novo acute myelogenous leukemias. *Oncogene*. 2006;25:1434–1436.
41. Dohner K, Du J, Corbacioglu A, et al. JAK2V617F mutations as cooperative genetic lesions in t(8;21)-positive acute myeloid leukemia. *Haematologica*. 2006;91(11 SE-Letters to the Editor):1569–1570.
42. Babon JJ, Kershaw NJ, Murphy JM, et al. Suppression of cytokine signaling by SOCS3: characterization of the mode of inhibition and the basis of its specificity. *Immunity*. 2012;36:239–250.
43. Boyle K, Egan P, Rakar S, et al. The SOCS box of suppressor of cytokine signaling-3 contributes to the control of G-CSF responsiveness in vivo. *Blood*. 2007;110:1466–1474.
44. Zhang H, Coblentz C, Watanabe-Smith K, et al. Gain-of-function mutations in granulocyte colony–stimulating factor receptor (CSF3R) reveal distinct mechanisms of CSF3R activation. *J Biol Chem*. 2018;293:7387–7396.
45. Irby RB, Yeatman TJ. Role of Src expression and activation in human cancer. *Oncogene*. 2000;19:5636–5642.
46. Lim Y, Gondek L, Li L, et al. Integration of Hedgehog and mutant FLT3 signaling in myeloid leukemia. *Sci Transl Med*. 2015;7:291ra96.
47. Lim Y, Matsui W. Hedgehog signaling in hematopoiesis. *Crit Rev Eukaryot Gene Expr*. 2010;20:129–139.
48. Jamieson C, Martinelli G, Papayannidis C, et al. Hedgehog pathway inhibitors: a new therapeutic class for the treatment of acute myeloid leukemia. *Blood Cancer Discov*. 2022;1:134–145.
49. Sadarangani A, Pineda G, Lennon KM, et al. GLI2 inhibition abrogates human leukemia stem cell dormancy. *J Transl Med*. 2015;13:1.
50. US Food and Drug Administration. Highlights of prescribing information: DAURISMO™ 2018. Published 2018. Available at: https://www.accessdata.fda.gov/drugsatfda_docs/label/2018/210656s000lbl.pdf. Accessed June 5, 2022.
51. European Medicines Agency. Summary of opinion (initial authorisation): Daurismo (glasdegib). Published 2020. Available at: https://www.ema.europa.eu/en/documents/smop-initial/chmp-summary-positive-opinion-daurismo_en.pdf. Accessed June 5, 2022.
52. Pan D, Li Y, Li Z, et al. Gli inhibitor GANT61 causes apoptosis in myeloid leukemia cells and acts in synergy with rapamycin. *Leuk Res*. 2012;36:742–748.
53. Long B, Wang LX, Zheng F, et al. Targeting GLI1 suppresses cell growth and enhances chemosensitivity in CD34+ enriched acute myeloid leukemia progenitor cells. *Cell Physiol Biochem*. 2016;38:1288–1302.
54. Chien W, Sudo M, Ding LW, et al. Functional genome-wide screening identifies targets and pathways sensitizing pancreatic cancer cells to dasatinib. *J Cancer*. 2018;9:4762–4773.
55. Okabe S, Tauchi T, Tanaka Y, et al. Effects of the hedgehog inhibitor GDC-0449, alone or in combination with dasatinib, on BCR-ABL-positive leukemia cells. *Stem Cells Dev*. 2012;21:2939–2948.
56. Larsen LJ, Møller LB. Crosstalk of hedgehog and mTORC1 pathways. *Cells*. 2020;9:2316.
57. Han L, Schuringa JJ, Mulder A, et al. Dasatinib impairs long-term expansion of leukemic progenitors in a subset of acute myeloid leukemia cases. *Ann Hematol*. 2010;89:861–871.
58. Bantscheff M, Eberhard D, Abraham Y, et al. Quantitative chemical proteomics reveals mechanisms of action of clinical ABL kinase inhibitors. *Nat Biotechnol*. 2007;25:1035–1044.
59. Rix U, Hantschel O, Dü Rnberger G, et al. Chemical proteomic profiles of the BCR-ABL inhibitors imatinib, nilotinib, and dasatinib reveal novel kinase and nonkinase targets. *Blood*. 2007;110:4055–4063.
60. Li J, Rix U, Fang B, et al. A chemical and phosphoproteomic characterization of dasatinib action in lung cancer. *Nat Chem Biol*. 2010;6:291–299.
61. Choi KM, Cho E, Bang G, et al. Activity-based protein profiling reveals potential dasatinib targets in gastric cancer. *Int J Mol Sci*. 2020;21:9276–9214.